Tribology Letters (2018) 66:54
https://doi.org/10.1007/s11249-018-1005-2

ORIGINAL PAPER

Tip-Enhanced Raman Spectroscopy Studies on Amorphous Carbon Films and Carbon Overcoats in Commercial Hard Disk Drives

Andreas Rosenkranz[1] · Lindsay Freeman[2] · Benjamin Suen[1] · Yeshaiahu Fainman[2] · Frank E. Talke[1]

Received: 14 January 2018 / Accepted: 21 February 2018

Abstract
Far-field Raman spectroscopy and tip-enhanced Raman spectroscopy were used to investigate 20-nm-thick amorphous carbon films and 3-nm-thick carbon overcoats of commercial hard disk drives. Enhancement of the Raman signal on both samples was observed indicating the activation of surface plasmons. The largest enhancement was found for the 3-nm-thick carbon overcoat of a commercial hard disk suggesting that the chemistry of nanometer-thick carbon films can be studied using tip-enhanced Raman spectroscopy with high sensitivity and resolution.

Keywords Hard disk drives · Carbon overcoats · Diamond-like carbon · Tip-enhanced Raman spectroscopy

1 Introduction

In the last decade, tip-enhanced Raman spectroscopy has been utilized for sensing and chemical imaging of materials and especially carbon materials on the nanoscale [1, 2]. In order to realize tip-enhanced Raman spectroscopy, a Raman spectrometer is coupled with either an atomic force microscope, a shear force microscope or a scanning tunneling microscope [3]. The laser light of the Raman spectrometer is focused on the metalized tip of any of those scanning devices. If the tip is in close proximity of the surface of interest, the metalized tip acts as an antenna for light, inducing surface plasmons and consequently enhancing the emitted electric field [4–6]. Due to the large field enhancement encountered, materials known to be weak Raman scatterers can be probed with high resolution. Hayazawa et al. investigated single-wall carbon nanotubes and amorphous carbon films by tip-enhanced Raman spectroscopy and compared the respective far-field spectra with the tip-enhanced signals. For single-wall carbon nanotubes, they demonstrated a selective enhancement of the G-peak, while amorphous carbon exhibited a more pronounced D-peak [7]. Chen et al. verified a spatial resolution of 1.7 nm using tip-enhanced Raman spectroscopy with a scanning tunneling microscope and individual carbon nanotubes as probed material. Local defects, bundling effects and different types of carbon nanotubes were imaged with high resolution. In addition, the authors showed a stronger enhancement of the G-peak compared to the D-peak [8]. Using a tip-enhanced Raman setup based upon a scanning tunneling microscope, Liao et al. could verify a spatial resolution of 0.7 nm for individual carbon nanotubes. The high resolution makes tracking of strain-induced structural changes possible. Bending experiments on individual carbon nanotubes and in situ tip-enhanced Raman spectroscopy measurements revealed a split up of the G-peak which depends on the degree of deformation [9]. Saito et al. studied the influence of the polarization of the exciting laser source on the resulting spectra of single-wall carbon nanotubes recorded by tip-enhanced Raman spectroscopy. The polarization was varied between s-polarization (parallel to the sample plane) and p-polarization (perpendicular to the sample plane). They observed a selective enhancement of the G-peak using s-polarized laser light, while p-polarized light enhances more the radial breathing mode. This selective enhancement of vibrational modes can be explained by the connection of the laser polarization and the orientation of vibrational moments on the molecular level. Comparing far- and near-field measurements, Saito et al. [10] observed a maximum enhancement factor of 2.5 for the G-peak. As demonstrated in the studies discussed above, tip-enhanced Raman spectroscopy is a powerful tool

✉ Andreas Rosenkranz
arosenkranz@ucsd.edu

[1] Center for Memory and Recording Research, UC San Diego, La Jolla, CA 92093, USA

[2] Electrical and Computer Engineering Department, UC San Diego, La Jolla, CA 92093, USA

Published online: 01 March 2018

for studying changes in structure and chemistry of carbon nanoparticles and/or nanometer-thick carbon films with high accuracy and sensitivity.

In this study, 20-nm-thick amorphous carbon films consisting of sp^2- and sp^3-hybridized carbon were investigated by tip-enhanced Raman spectroscopy. In addition, carbon overcoats used in hard disk drives with a film thickness of two to three nanometers were studied using tip-enhanced Raman spectroscopy. Our goal is to verify that tip-enhanced Raman spectroscopy can be used to characterize structural changes in nanometer-thick carbon films with mixed sp^2–sp^3-hybridization as used for carbon overcoats in commercial hard disk drives.

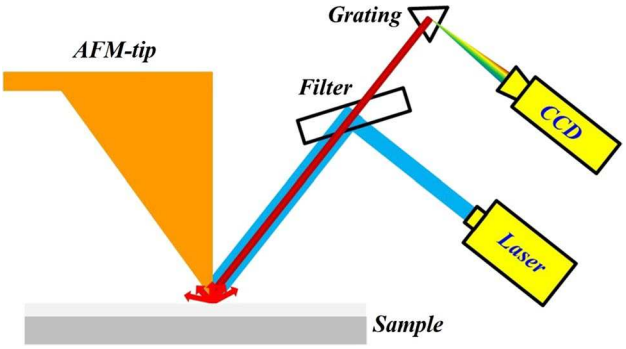

Fig. 1 Schematic illustration of the used tip-enhanced Raman spectroscopy system consisting of an atomic force microscope and a Raman spectrometer

2 Experimental

2.1 Plasma-enhanced Chemical Vapor Deposition

Amorphous carbon films with a thickness of 20 nm were deposited on a silicon wafer using the following procedure. First, the wafer was cleaned and stripped of its native oxide layer. The silicon wafers used in this experiment were metal-backed *p*-type < 100 > wafers. The native oxide layer was removed by dipping the wafer in a 2% hydrofluoric acid bath for 5 min, and a 20-nm-thick amorphous carbon film was deposited using plasma-enhanced chemical vapor deposition. The films were deposited on the polished bare silicon side of the wafer. An Oxford Plasmalab 80 was used as deposition tool. The amorphous carbon was deposited by decomposing methane at 100 mTorr pressure, 20 °C temperature and 50 standard cubic centimeters per minute flow rate using 250 W of RF power.

2.2 Commercial Hard Disk Drive

The hard disk drive media was cut from a 3.5-inch aluminum disk intended for use in production drives. The carbon overcoat on the media was about 2.5 nm thick and was fabricated by conventional sputtering techniques. The carbon overcoat is protected with a monolayer of perfluoropolyether-based lubricant of approximately 1.5 nm thickness.

2.3 Tip-Enhanced Raman Spectroscopy

Tip-enhanced Raman measurements were performed using confocal Raman spectrometer (Renishaw inVia) coupled with an atomic force microscope (Nanonics MV 2000), as schematically shown in Fig. 1.

A 532-nm excitation laser was used with acquisition time of 60 s. The optics within the Raman spectrometer consist of a 130 cm^{-1} cutoff EDGE filter for the 532-nm laser with a 2400 grating and a 1024 pixel deep-depletion CCD. The atomic force microscope was controlled by two piezoelectric drivers, one that controlled the movement of the sample stage in *X*–*Y* and one that controlled the tip in *X*–*Y*–*Z*. The tips were cantilevered tapered glass micropipettes designed for tip-enhanced Raman measurements with a gold nanoparticle placed at the end of the tip. The tip was mounted on a tuning fork. The tuning fork was used to control the distance between the tip and the sample surface. The tip was manually moved to be within several microns of the surface, and the SPM controller moved the tip into contact with the surface using the resonance frequency of the tuning fork for feedback.

Tip-enhanced Raman spectroscopy measurements (near-field) were performed with the laser being focused on the gold tip. For far-field measurements, the tip was retracted approximately 200 nm from the surface and moved laterally out of range by more than 50 microns. The far-field measurements were acquired at the same sample location as the near-field measurements. To obtain new locations on the same sample, the lower piezoelectric driver was used to move the sample to the new position while the tip was out-of-contact with the surface. The location of the tip with respect to the laser was adjusted using continuous Raman acquisitions. Both far-field and near-field measurements were performed at each location.

3 Results and Discussion

Far-field Raman spectra of all samples (carbon-coated silicon and carbon-coated hard disk surface) were first obtained in order to determine the reference state. Figure 2a shows the corresponding far-field measurements for the 20-nm amorphous carbon film while Fig. 2b shows the far-field measurements for the 3-nm carbon overcoat in a hard disk drive. Figure 2c, d shows the corresponding far-field measurements for both samples using a longer acquisition time of 3 min.

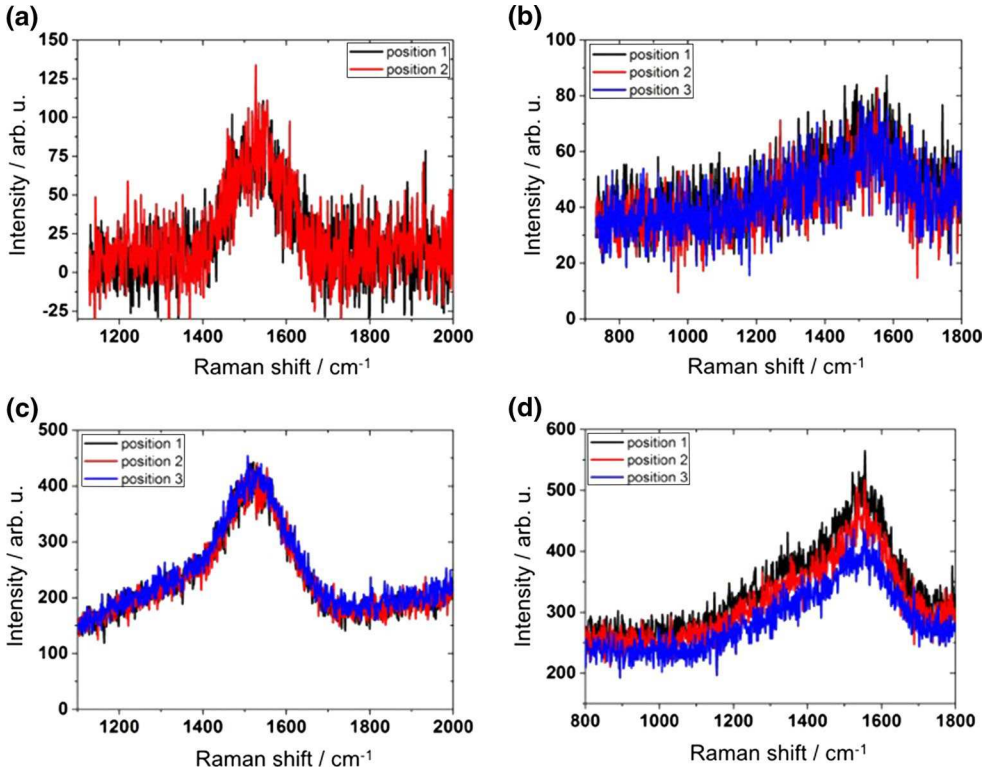

Fig. 2 Far-field Raman spectra for **a** a 20-nm amorphous carbon and **b** a 3-nm carbon overcoat of a hard disk drive measured at different positions. **c** and **d** shows the far-field Raman spectra for a 20-nm amorphous carbon and a 3-nm carbon overcoat of a hard disk drive, respectively, using a longer acquisition time of three minutes

As can be seen in Fig. 2a, b, the spectra for the 20-nm amorphous carbon film and the 3-nm carbon layer of the hard disk drive are similar. Both spectra show a broad Raman peak centered at around 1500 cm^{-1}. The broad Raman peak is typical for amorphous carbon films and is a convolution of the D-peak and G-peak. Line broadening can be correlated with the existing cluster size and the cluster distribution in amorphous carbon films. Moreover, residual stresses in the film due to fabrication can also contribute to a broadened Raman peak [11]. Additionally, it can be observed that both samples give a weak Raman signal with low intensity and poor signal-to-noise ratio. This is because of the small carbon layer thickness of approximately 20 and 3 nm, respectively, and the used experimental conditions, which were necessary to allow a direct comparison between far-field and near-field measurements [12, 13]. Furthermore, the signal-to-noise ratio can be influenced by foreign atoms such as hydrogen or nitrogen incorporated in the carbon network during fabrication [12]. The signal-to-noise ratio and the Raman spectra can be improved by using longer acquisition times. Figure 2c, d shows the far-field Raman spectra of the 20-nm amorphous carbon film and the 3-nm carbon overcoat in a hard disk drive, respectively, measured with an increased acquisition time of 3 min. Similar to Fig. 2a, b, the spectra demonstrate a broad peak centered at around 1500 cm^{-1} (convolution of the D-peak and G-peak) with an increased intensity and improved signal-to-noise ratio. This peak can be deconvoluted and structural information can be gained.

Figure 3 shows a comparison of the far-field and near-field measurements for the amorphous carbon film with a thickness of 20 nm [(a) and (b)] and the 3-nm carbon overcoat of a hard disk [(c) and (d)]. Far-field and near-field spectra were taken at the same position keeping all parameters constant. Two different measurements are shown in order to demonstrate the repeatability of the obtained results.

The far-field spectra for the amorphous carbon film and the carbon overcoat of a hard disk show a weak signal with a broad peak located at approximately 1540 cm^{-1}. On the other hand, the respective near-field measurements show a completely different behavior. In the case of amorphous carbon, two distinct peaks can be observed, located at 1348 and 1605 cm^{-1}, respectively. These peaks can be related to the D-peak and G-peak of typical carbon systems. It is apparent that the near-field spectrum is enhanced compared to the far-field measurement. In addition to these two peaks, a number of additional peaks and shoulders arising at different Raman shift values can be observed. The appearance of these peaks is in good agreement with Veres et al., who studied amorphous carbon films and hydrogenated amorphous carbon films by surface-enhanced Raman spectroscopy. They explained the appearance of those additional peaks by the "composite character" of the D-peak and G-peak. The D-peak and G-peak can be regarded as inhomogeneously broadened bands consisting of a large number of

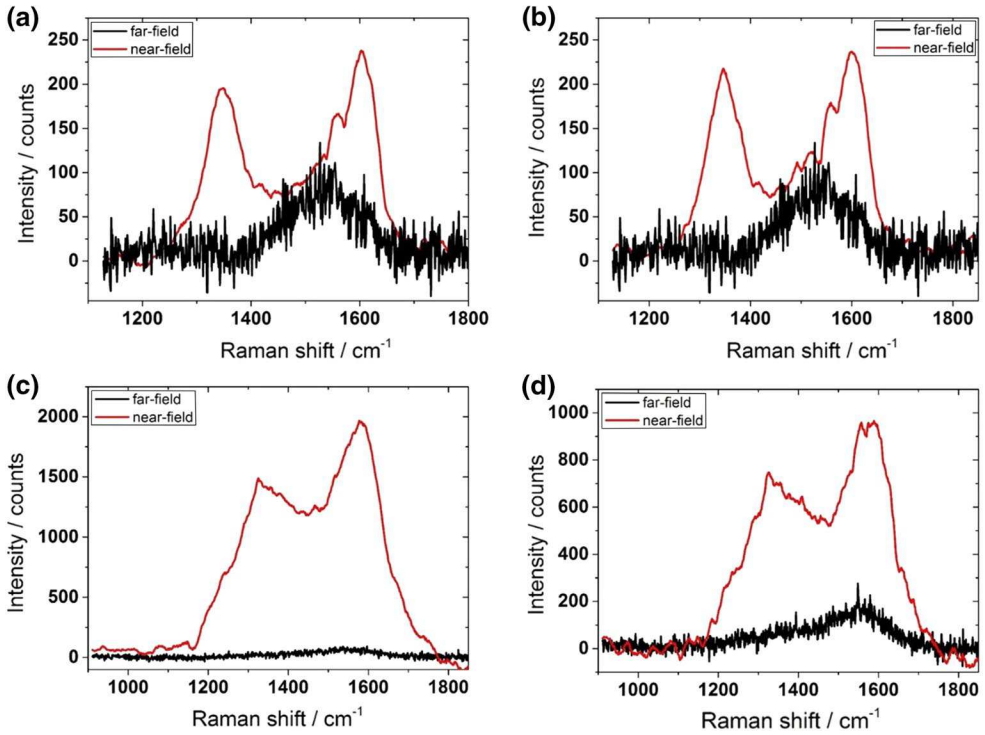

Fig. 3 Near-field Raman spectra for the 20-nm amorphous carbon film (**a**) and (**b**) and the 3-nm-thick carbon overcoat of a commercial hard disk (**c**) and (**d**) obtained at two different positions

individual components. The concentration and Raman cross section of each individual structural unit as well as the distance between the tip and the structural unit determine which unit is selectively enhanced [14]. Kudelski and Pettinger [15] pointed out that the narrow Raman peaks can be traced back to local variations in the carbon configuration. For the 20-nm-thick amorphous carbon film, the maximum enhancement factor for the D-peak and G-peak is about 8 and 3.5, respectively.

In order to calculate the enhancement based upon the enhancement factor, the different spot sizes of the far-field and near-field measurements need to be taken into consideration. This can be calculated using the following equation

$$\mathrm{EF} = C\frac{V_{\mathrm{focus}}}{V_{\mathrm{tip}}}, \tag{1}$$

where V_{focus} represents the volume of the excited far field, V_{tip} represents the volume of the excited field near the tip and C represents the contrast between the far-field and the near-field measurements. Assuming a cylindrical volume field from the laser, we can express Eq. (1) as

$$\mathrm{EF} = C\frac{\pi r_{\mathrm{far}}^2 h_{\mathrm{far}}}{\pi r_{\mathrm{tip}}^2 h_{\mathrm{tip}}}, \tag{2}$$

where r_{far} denotes the radius of the laser spot in the far field, h_{far} represents the height of the far-field focus, r_{tip} represents the radius of the laser sport in the near field and h_{tip} represents the height of the near-field focus. For the far field, r_{far} and h_{far} are about 3 µm and 500 nm, respectively, while for the near field, r_{tip} and h_{tip} are roughly 100 and 20 nm, respectively. Based upon Eq. (2), the enhancement for the D-peak and G-peak in the case of the 20-nm amorphous carbon film can be calculated to be approximately 180×10^3 and 78×10^3, respectively.

In the case of the 3-nm carbon layer of a hard disk, similar experimental results were obtained. The near-field spectra show a significant enhancement with a pronounced D-peak and G-peak at a Raman shift of 1350 and 1582 cm^{-1}, respectively. The maximum enhancement factors are about 47 and 36 for the D-peak and G-peak. This leads to an enhancement by 1057×10^3 for the D-peak and 810×10^3 for the G-peak.

Based upon Fig. 3, it is apparent that the near-field spectra for both samples are enhanced compared to the far-field measurements and that the signal-to-noise ratio is improved. In order to explain these observations, different aspects have to be taken into consideration. The two samples may differ in the degree of amorphicity and the ratio of sp^2–sp^3 hybridization, which can influence the measurements and signal-to-noise ratio. The surface roughness of the 3-nm-thick carbon overcoat of the hard disk drive is expected to

be lower, which can improve the enhancement and reduce the signal-to-noise ratio. The 3-nm carbon overcoat of the hard disk drive is fabricated in a facility dedicated to carbon deposition. Consequently, the influence of foreign atoms on the resulting Raman signal is reduced. In contrast, the sputter facility used for the 20-nm carbon coating is also used for the deposition of various other materials. As a consequence, foreign atoms can play a more pronounced role in reducing possible enhancement as well as affecting the signal-to-noise ratio. Another aspect that needs to be considered is the layout of the individual samples. The 20-nm amorphous carbon film consists of a silicon substrate and a 20-nm amorphous carbon film on the top surface. A hard disk drive typically has a multilayer structure including a lubricant layer on the top surface, followed by a 3-nm carbon overcoat and several other layers magnetic and non-magnetic layers. Some of these layers can contain thin films with platinum group metals and alloys of those metals. Those metals and alloys are normally plasmonically inactive. However, when placing a near-field probe above the surface, the metallic layer may help create a gap mode between the tip and the surface, thereby enhancing the Raman signal [16].

The results presented for amorphous carbon and the hard disk overcoat underline the great advantage of using near-field techniques such as tip-enhanced Raman spectroscopy for the characterization of films with a thickness in the nanometer range. A small carbon layer thickness of 20 or 3 nm can lead to a poor signal-to-noise ratio and rather weak far-field signal. An increase in the acquisition time significantly improves the Raman signal as well as the signal-to-noise ratio. However, longer acquisition times are not recommended since this increases the probability to induce structural changes in thin carbon films by the measurement itself. Due to the signal enhancement in tip-enhanced Raman spectroscopy, materials known as weak Raman scatterers and nanometer-thick films can be investigated with high sensitivity using shorter acquisition times. The increased sensitivity and gain in intensity allow for an accurate deconvolution of the D-peak and G-peak for carbon materials. This in turn enables us to study structural changes such as graphitization and amorphization precisely. Furthermore, the spatial resolution of tip-enhanced Raman spectroscopy is on the order of 50 nm. Due to exact knowledge of the tip location during the measurements, this technique can be used to study induced chemical changes with a high spatial resolution. In heat-assisted magnetic recording, high temperatures, high heating and cooling rates (approx. 10^{11}–10^{12} K/s) and thermal cycling are encountered [17, 18]. This can lead to significant changes of material properties including material degradation and oxidation of the carbon overcoat and the lubricant protecting the magnetic medium [19]. With respect to the carbon overcoat, laser heating may result in oxidation, graphitization, amorphization or a change in the sp^2/sp^3-ratio [17, 20, 21]. Thus, tip-enhanced Raman spectroscopy can serve as a unique characterization technique since it allows the investigation of material changes on a nanometer scale and thereby permits the correlation between a change in materials properties with the tribological performance and reliability of a hard disk drive. Especially for heat-assisted magnetic recording, tip-enhanced Raman spectroscopy can be considered as the right tool due to the accessible scale and high sensitivity, which is needed to successfully probe nanometer-thick carbon films. In order to capture thermally induced changes in the 1.5-nm-thick lubricant layer, it may be necessary to use tip-enhanced IR-spectroscopy.

4 Conclusions

Far-field Raman spectroscopy and tip-enhanced Raman spectroscopy were used to investigate 20-nm-thick amorphous carbon films fabricated by plasma-enhanced chemical vapor deposition and 3-nm-thick carbon overcoats of hard disk drives. From the experimental results, we conclude:

1. The far-field Raman spectrum for both samples was weak and exhibited a poor signal-to-noise ratio due to the small carbon thickness.
2. Near-field spectra were observed for all samples investigated and the recorded near-field Raman spectra demonstrated good repeatability.
3. Significant enhancement using tip-enhanced Raman spectroscopy was observed for all samples tested. The largest enhancement factor was found for the hard disk drive carbon overcoat leading to an enhancement on the order of 10^6.
4. In addition to the well-known D-peak and G-peak for carbon systems, additional peaks arising as shoulders were observed for both samples. The appearance of those peaks is well correlated with published work on similar material systems performed using surface-enhanced Raman spectroscopy.

Based upon the results presented in this paper, it is apparent that tip-enhanced Raman spectroscopy is a promising method for the investigation of thermally induced structural changes in the carbon overcoat of hard disk drives used for heat-assisted magnetic recording.

Acknowledgements Andreas Rosenkranz acknowledges the Feodor Lynen Fellowship of the Alexander von Humboldt foundation. This work was supported by the National Science Foundation (NSF) (Grants CBET-1704085, DMR-1707641, ECCS-1405234 and ECCS-1507146) and the Cymer Corporation. This work was performed in part at the San Diego Nanotechnology Infrastructure (SDNI) of UCSD, a member of the National Nanotechnology Coordinated Infrastructure, which is supported by the NSF (Grant ECCS-1542148).

References

1. Schmid, T., Opilik, L., Blum, C., Zenobi, R.: Nanoscale chemical imaging using tip-enhanced Raman spectroscopy: a critical review. Angew. Chem. Int. Ed. **52**, 5940–5954 (2013)
2. Blum, C., Opilik, L., Atkin, J.M., Braun, K., Kämmer, S.B., Kravstov, V., Kumar, N., Lemeshko, S., Li, J.F., Luszcz, K., Maleki, T., Meixner, A.J., Minne, S., Raschke, M.B., Ren, B., Rogalski, J., Roy, D., Stephanidis, B., Wang, X., Zhang, D., Zhong, J.H., Zenobi, R.: Tip-enhanced Raman spectroscopy—an interlaboratory reproducibility and comparison study. J. Raman Spectrosc. **45**, 22–31 (2014)
3. Stadler, J., Schmid, T., Zenobi, R.: Developments in and practical guidelines for tip-enhanced Raman spectroscopy. Nanoscale **4**, 1856–1870 (2012)
4. Pettinger, B., Schambach, P., Villagomez, C.J., Scott, N.: Tip-enhanced Raman spectroscopy: near-fields acting on a few molecules. Annu. Rev. Phys. Chem. **63**, 379–399 (2012)
5. Berweger, S., Atkin, J.M., Olmon, R.L., Raschke, M.B.: Adiabatic tip-plasmon focusing for nano-Raman spectroscopy. J. Phys. Chem. Lett. **1**, 3427–3432 (2010)
6. Berweger, S., Atkin, J.M., Olmon, R.L., Raschke, M.B.: Light on the tip of a needle: plasmonic nanofocusing for spectroscopy on the nanoscale. J. Phys. Chem. Lett. **3**, 945–952 (2012)
7. Hayazawa, N., Yano, T., Watanabe, H., Inouye, Y., Kawata, S.: Detection of an individual single-wall carbon nanotube by tip-enhanced near-field Raman spectroscopy. Chem. Phys. Lett. **376**, 174–180 (2003)
8. Chen, C., Hayazawa, N., Kawata, S.: A 1.7 nm resolution chemical analysis of carbon nanotubes by tip-enhanced Raman imaging in the ambient. Nat. Commun. **4**, 1–5 (2014)
9. Liao, M., Jiang, S., Hu, C., Zhang, R., Kuang, Y., Zhu, J., Zhang, Y., Dong, Z.: Tip-enhanced Raman spectroscopic imaging of individual Carbon nanotubes with subnanometer resolution. Nano Lett. **16**, 4040–4046 (2016)
10. Saito, Y., Hayazawa, N., Kataura, H., Murakami, T., Tsukagoshi, K., Inouye, Y., Kawata, S.: Polarization measurements in tip-enhanced Raman spectroscopy applied to single-walled carbon nanotubes. Chem. Phys. Lett. **410**, 136–141 (2005)
11. Schwan, J., Ulrich, S., Batori, V., Ehrhardt, H., Silva, S.R.P.: Raman spectroscopy on amorphous carbon films. J. Appl. Phys. **80**, 440–447 (1996)
12. Ferrari, A.C., Robertson, J.: Raman spectroscopy of amorphous, nanostructured, diamond-like carbon, and Nanodiamond. Philos. Trans. R. Soc. Lond. A **362**, 2477–2512 (2004)
13. Chu, P.K., Li, L.: Characterization of amorphous and nanocrystalline carbon films. Mater. Chem. Phys. **96**, 253–277 (2006)
14. Veres, M., Fuele, M., Toth, S., Koos, M., Pocsik, I.: Surface enhanced Raman scattering (SERS) investigation of amorphous carbon. Diam. Relat. Mater. **13**, 1412–1415 (2004)
15. Kudelski, A., Pettinger, B.: SERS on carbon chain segments: monitoring locally surface chemistry. Chem. Phys. Lett. **321**, 356–362 (2000)
16. Katsuyoshi, I., Sato, J., Uosaki, K.: Surface-enhanced scattering at well-defined single crystalline faces of platinum-group metals induced by gap-mode plasmon excitation. J. Photochem. Photobiol. A **221**, 175–180 (2011)
17. Rottmayer, R.E., Barta, S., Buechel, D., Challener, W.A., Hohlfeld, J., Kubota, Y., Li, L., Lu, B., Mihalcea, C., Mountfield, K., Pelhos, K.: Heat-assisted magnetic recording. IEEE Trans. Magn. **42**, 2417–2421 (2006)
18. Kryder, M.H., Gage, E.C., McDaniel, T.W., Challener, W.A., Rottmayer, R.E., Ju, G., Hsia, Y.T., Erden, M.F.: Heat assisted magnetic recording. Proc. IEEE **96**, 1810–1835 (2008)
19. Marchon, B., Guo, X.C., Pathem, B.K., Rose, F., Dai, Q., Feliss, N., Schreck, E., Reiner, J., Mosendz, O., Takano, K., Do, H., Bruns, J., Saito, Y.: Head-disk interface materials issues in heat-assisted magnetic recording. IEEE Trans. Magn. **50**, 3300607 (2014)
20. Pathem, B.K., Guo, X.C., Rose, F., Wang, N., Komvopoulos, K., Schreck, E., Marchon, B.: Carbon overcoat oxidation in heat-assisted magnetic recording. IEEE Trans. Magn. **49**, 3721–3724 (2013)
21. Xu, S., Sinha, S., Rismaniyazdi, E., Wolf, C., Dorsey, P., Knigge, B.: Effect of carbon overcoat on heat-assisted magnetic recording performance. IEEE Trans. Magn. **51**, 3301805 (2015)